# The International Journal of
# Robotics Research

**Analysis of Multifingered Hands**
Jeffrey Kerr and Bernard Roth

The online version of this article can be found at:

Published by:

**⑤SAGE**

On behalf of:

**ijrr**

Multimedia Archives

Additional services and information for *The International Journal of Robotics Research* can be found at:

**Email Alerts:** http://ijr.sagepub.com/cgi/alerts

**Subscriptions:** http://ijr.sagepub.com/subscriptions

**Reprints:** http://www.sagepub.com/journalsReprints.nav

**Permissions:** http://www.sagepub.com/journalsPermissions.nav

**Citations:** http://ijr.sagepub.com/content/4/4/3.refs.html

>> Version of Record - Jan 1, 1986

What is This?

# Jeffrey Kerr

General Motors Research Laboratories,
Warren, Michigan

# Bernard Roth

Stanford University
Stanford, California 94305

# Analysis of Multifingered Hands

## Abstract

*This paper discusses three fundamental problems relating to grasping and manipulating objects within an articulated, multifingered hand: determining how hard to squeeze an object in order to ensure a secure grasp, determining the finger-joint motions required to produce a desired motion of the object, and determining the workspace of the hand.*

*Squeezing the object, or the application of* internal grasp forces, *is reduced to a linear programming problem which considers friction and joint torque limit constraints. The relationship between the finger-joint motions and the motion of the object, for the case of pure rolling between the fingertips and the object, is formulated as a set of differential equations. The* total workspace *for a hand is determined for special cases of planar and spatial hands.*

## Introduction

Articulated, multifingered hands have the potential for solving some of the problems encountered in manipulating objects with robotic arms. Ultimately, such hands will possess the sensitivity and dexterity to greatly extend the class of tasks that can be performed by autonomous manipulation systems.

Manipulating objects within a multifingered hand is, of course, much more complicated than simply manipulating an object rigidly attached to the end of a six-axis robot arm. Not only are the kinematic relationships between the finger-joint motions and the object motion complicated, but the hand must also firmly grasp the object during the course of the motion. Planning motions of an object within a hand is also complicated because the range of possible motions is usually rather restricted and because the motions are strongly a function of the size of the object.

Although much early work has been done on the mechanics of manipulators (for example, Roth 1975), only recently has there been a growing interest in multifingered, dexterous hands (Hollerbach 1982; Salisbury 1982; Holzmann and McCarthy 1985).

This paper treats three of the fundamental problems encountered in grasping and manipulating objects within a multifingered hand. The first of these problems is that of determining how hard to squeeze an object with the fingers in order to ensure that the object is grasped stably. This squeezing of the object is formally termed the application of internal grasp forces. This part of our work follows closely on Salisbury 1982, Salisbury and Craig 1981, and to a lesser extent Ohwovoriole 1980. The second problem discussed is that of determining the finger-joint motions required to produce some desired motion of the object. In particular, we examine this problem under the condition that there is pure rolling between each of the fingertips and the object. The last problem discussed is that of determining the ranges of motion of an object grasped by a hand. The ranges of motion in different directions form what is known as the workspace of the hand. Here, we develop the workspace of a restricted set of hands, but the concepts may be extended to more general hands.

## 1. Selection of Internal Grasp Forces

When a rigid object is grasped stably[1] by a set of fingertips, as shown in figure 1, we can write force and moment balance equations relating external environ-

---

1. There have been various technical definitions of stability (see, for example, Hanafusa and Asada 1977). We mean simply the ability of the fingers to prevent the object from undergoing unwanted movements under the simplifying assumptions of our model.

Fig. 1. An object in a stable grasp.
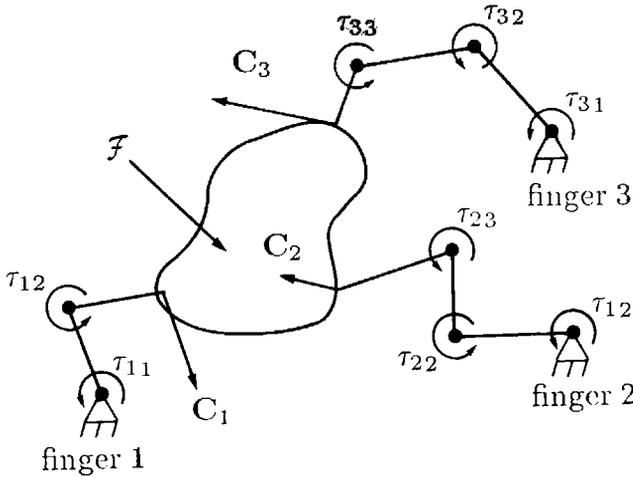


mental forces and moments applied to the object to the components of the forces and moments applied to the object by all the fingertips. If the environmental force and moment components are described by the $6 \times 1$ generalized force vector $\mathcal{F}$ and the components of the finger contact forces and moments are assembled into the $n \times 1$ vector C, the force balance can be described by the linear equation

$$-\mathcal{F} = \mathbf{WC}, \qquad (1)$$

where W is a $6 \times n$ matrix. This is essentially the same relationship discussed in Salisbury 1982.

In general, the total number of force and moment components exerted by the fingertips will be greater than 6, and the object will be overconstrained. If the object were supported by passively constrained fingers, the statically indeterminate force and moment components of C would have to be determined by examining the flexibility of the object and of the fingers. If the fingers have enough joints so that we can actively control the components of the contact forces, however, we can explicitly choose the values of the statically indeterminate components, as long as certain friction constraints are met. These statically indeterminate components are called *internal grasp forces.*

In general, for a given value of $\mathcal{F}$, there will not be a unique solution for C from equation 1. Any solution for C can be broken up into the two vectors $\mathbf{C}_p$ and $\mathbf{C}_h$

such that

$$\mathbf{C} = \mathbf{C}_p + \mathbf{C}_h, \qquad (2)$$

where $\mathbf{C}_p$ is orthogonal to $\mathbf{C}_h$ and where $\mathbf{C}_h$ lies in the null space of W. $\mathbf{C}_p$ can be determined through the use of the right generalized inverse of W (see, for example, Strang 1976):

$$\mathbf{C}_p = -\mathbf{W}_R^+\mathcal{F}. \qquad (3)$$

The vector $\mathbf{C}_h$ corresponds to the internal grasp forces.

If a set of orthonormal basis vectors which span the null space of W are assembled into the columns of the matrix N, then $\mathbf{C}_h$ can be written in terms of the $m \times 1$ vector $\lambda$ as

$$\mathbf{C}_h = \mathbf{N}\lambda. \qquad (4)$$

$m$ is the dimension of the null space of W. The magnitudes of the internal grasp forces are the elements of $\lambda$.

### Friction Constraints

If an object is grasped in a manner whereby the finger contact friction is needed to maintain a stable grasp, friction at the contacts must be active and the available friction force limits must not be exceeded. For friction to be active, the component of the contact force normal to the object's surface at each such contact, $c_{i\,\text{normal}}$, must be positive. For each contact, we have the constraint

$$c_{i\,\text{normal}} \geq 0, \qquad (5)$$

where the subscript $i$ refers to the $i$th contact.

We must also ensure that the tangential components of the contact forces do not exceed the magnitude of the equilibrating friction force. Using a Coulomb friction model, this constraint is written as

$$\sqrt{c_{ix}^2 + c_{iy}^2} \leq \mu c_{i\,\text{normal}}, \qquad (6)$$

where $\mu$ is the coefficient of static friction. Equation 6, with $c_{ix}$, $c_{iy}$, and $c_{i\,\text{normal}}$ as mutually orthogonal components, describes a cone. The friction limits can be linearized by approximating this cone with a set of

*Fig. 2. Example 1.*

planes tangent to the cone. If we choose to use four planes, the linear approximation to equation 6 is written as the set of equations

$$c_{ix} + \mu c_{i\,\text{normal}} \geq 0,$$

$$c_{ix} - \mu c_{i\,\text{normal}} \leq 0,$$

$$c_{iy} + \mu c_{i\,\text{normal}} \geq 0,$$ (7)

$$c_{iy} - \mu c_{i\,\text{normal}} \leq 0.$$

The value of $\mu$ can be adjusted downward to provide a more conservative approximation.

If the fingertip can apply a moment to the object about the surface normal, the torsional friction constraint can be written as

$$c_{i\,\text{torsion}} + \mu_t c_{i\,\text{normal}} \geq 0,$$ (8)

$$c_{i\,\text{torsion}} - \mu_t c_{i\,\text{normal}} \leq 0,$$

where $\mu_t$ is the torsional coefficient of static friction.

### Joint Torque Limits

Any physical hand will have limits on the torque that can be exerted at each of the finger joints. If the maximum torque values for all of the joints in the hand are assembled into the $n_{\text{joint}} \times 1$ vector $\mathcal{T}_{\text{max}}$, and the minimum values into the vector $\mathcal{T}_{\text{min}}$, the resulting limits on the components of **C** can be written as

$$\mathcal{J}^T \mathbf{C} \leq \mathcal{T}_{\text{max}},$$ (9)

$$\mathcal{J}^T \mathbf{C} \geq \mathcal{T}_{\text{min}},$$

where $\mathcal{J}$ is a Jacobian matrix for the entire hand. $\mathcal{J}^T$ can be determined by examining the relationship between the contact forces and moments at the fingertips and the finger joint torques required to produce them. In general, $\mathcal{J}$ will depend on the configuration of all the fingers.

Equations 5, 7, 8, and 9 form linear constraints on the elements of **C**. As such, they can be combined into the single vector inequality

$$\mathbf{AC} \geq \mathbf{P},$$ (10)
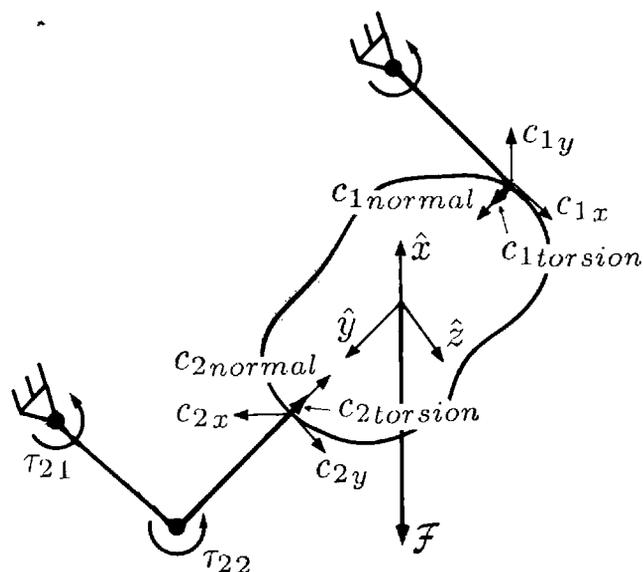
where the matrix **A** and the vector **P** contain the constants of the aforementioned constraints. Substituting in equations 2 and 4, equation 10 is rewritten as

$$\mathbf{AN}\lambda \geq \mathbf{P} - \mathbf{AC}_p.$$ (11)

Equation 11 shows how the vector of internal grasp forces, $\lambda$, can be determined so as to satisfy the friction limit constraints and the joint-torque limit constraints.

## THE CONSTRAINT POLYGON

Each of the scalar inequalities in equation 11 can be thought of as forming a hyperplane in $m$ space. Each hyperplane divides the space into a permissible half-space and an impermissible half-space. When all these inequalities are taken together, they will block off an $m$-dimensional polygonal region. Values of $\lambda$ that lie within this region will meet the friction limit constraints and the joint-torque limit constraints. If the fingers have a sufficient number of controllable joints, we will be able to explicitly choose a value of $\lambda$ that lies within this region and achieve a stable grasp.

The constraint polygon can be illustrated with the example shown in figure 2. The body is free to move spatially, but the fingers are constrained to move in

the plane of the paper. The fingers exert a *soft-finger* constraint on the object, where each fingertip can exert a force component normal to the surface, $c_{i\,normal}$, two force components tangential to the surface, $c_{ix}$ and $c_{iy}$, and a moment component about the surface normal, $c_{i\,torsion}$. $C$ is made up of all eight components (four for each contact).

For this example, the values of $W$, $\mathscr{E}$, and $\mathscr{T}$, described in terms of a reference frame located at the center of mass, are

$$W = \begin{bmatrix} 0 & 1 & 0 & 0 & 1 & 0 & 0 & 0 \\ 0 & 0 & 1 & 0 & 0 & 0 & -1 & 0 \\ 1 & 0 & 0 & 0 & 0 & 1 & 0 & 0 \\ -1 & 0 & 0 & 0 & 0 & 1 & 0 & 0 \\ 0 & 0 & 0 & 1 & 0 & 0 & 0 & -1 \\ 0 & 1 & 0 & 0 & -1 & 0 & 0 & 0 \end{bmatrix},$$

$$\mathscr{E}^T = \begin{bmatrix} 0 & 0 & -1 & 0 & 0 & 0 & 0 & 0 \\ 0 & 0 & 0 & 0 & 0 & -1 & 1 & 0 \\ 0 & 0 & 0 & 0 & 0 & -1 & 0 & 0 \end{bmatrix},$$

$$\mathscr{T} = \begin{bmatrix} 0 \\ 1 \\ 1 \\ 0 \\ 0 \\ 0 \end{bmatrix}.$$

An orthonormal basis for the null space of $W$ is

$$N = \begin{bmatrix} 0 & 0 \\ 0 & 0 \\ 0.707 & 0 \\ 0 & 0.707 \\ 0 & 0 \\ 0 & 0 \\ 0.707 & 0 \\ 0 & 0.707 \end{bmatrix}.$$

The first column of $N$ corresponds to equal values of the components $c_{1\,normal}$ and $c_{2\,normal}$. The second column of $N$ corresponds to equal values of the components $c_{1\,torsion}$ and $c_{2\,torsion}$. It is clear from figure 2 that either of these two combinations will result in no net force or moment upon the object.

The right generalized inverse of $W$ is found to be

$$W_R^+ = \begin{bmatrix} 0 & 0 & 0.5 & -0.5 & 0 & 0 \\ 0.5 & 0 & 0 & 0 & 0 & 0.5 \\ 0 & 0.5 & 0 & 0 & 0 & 0 \\ 0 & 0 & 0 & 0 & 0.5 & 0 \\ 0.5 & 0 & 0 & 0 & 0 & -0.5 \\ 0 & 0 & 0.5 & 0.5 & 0 & 0 \\ 0 & -0.5 & 0 & 0 & 0 & 0 \\ 0 & 0 & 0 & 0 & -0.5 & 0 \end{bmatrix}.$$

Using equation 3, $C_p$ is found to be

$$C_p = \begin{bmatrix} -0.5 \\ 0 \\ -0.5 \\ 0 \\ 0 \\ -0.5 \\ 0.5 \\ 0 \end{bmatrix}.$$

Combining the uniaxial constraints of equation 5, the friction constraints of equations 7 and 8, and the joint torque limit constraints of equation 9 produces the vector inequality

**6**

$$
\begin{bmatrix}
0 & 0 & 1 & 0 & 0 & 0 & 0 & 0 \\
0 & 0 & 0 & 0 & 0 & 0 & 1 & 0 \\
-1 & 0 & \mu & 0 & 0 & 0 & 0 & 0 \\
0 & -1 & \mu & 0 & 0 & 0 & 0 & 0 \\
0 & 0 & \mu_t & -1 & 0 & 0 & 0 & 0 \\
1 & 0 & \mu & 0 & 0 & 0 & 0 & 0 \\
0 & 1 & \mu & 0 & 0 & 0 & 0 & 0 \\
0 & 0 & \mu_t & 1 & 0 & 0 & 0 & 0 \\
0 & 0 & 0 & 0 & -1 & 0 & \mu & 0 \\
0 & 0 & 0 & 0 & 0 & -1 & \mu & 0 \\
0 & 0 & 0 & 0 & 0 & 0 & \mu_t & -1 \\
0 & 0 & 0 & 0 & 1 & 0 & \mu & 0 \\
0 & 0 & 0 & 0 & 0 & 1 & \mu & 0 \\
0 & 0 & 0 & 0 & 0 & 0 & \mu_t & 1 \\
0 & 0 & -1 & 0 & 0 & 0 & 0 & 0 \\
0 & 0 & 0 & 0 & 0 & -1 & 1 & 0 \\
0 & 0 & 0 & 0 & 0 & -1 & 0 & 0 \\
0 & 0 & 1 & 0 & 0 & 0 & 0 & 0 \\
0 & 0 & 0 & 0 & 0 & 1 & -1 & 0 \\
0 & 0 & 0 & 0 & 0 & 1 & 0 & 0
\end{bmatrix}
\begin{bmatrix}
c_{1x} \\ c_{1y} \\ c_{1\,normal} \\ c_{1\,torsion} \\ c_{2x} \\ c_{2y} \\ c_{2\,normal} \\ c_{2\,torsion}
\end{bmatrix}
\geq
\begin{bmatrix}
0 \\ 0 \\ 0 \\ 0 \\ 0 \\ 0 \\ 0 \\ 0 \\ 0 \\ 0 \\ 0 \\ 0 \\ 0 \\ 0 \\ \tau_{min} \\ \tau_{min} \\ \tau_{min} \\ -\tau_{max} \\ -\tau_{max} \\ -\tau_{max}
\end{bmatrix}.
$$

Choosing the specific values $\mu = 0.25$, $\mu_t = 0.5$, and $\tau_{max} = -\tau_{min} = 5.0$ for all joints, we get from equation 11

$$
\begin{bmatrix}
0.707 & 0 \\
0.707 & 0 \\
0.176 & 0 \\
0.176 & 0 \\
0.354 & -0.707 \\
0.176 & 0 \\
0.176 & 0 \\
0.354 & 0.707 \\
0.176 & 0 \\
0.176 & 0 \\
0.354 & -0.707 \\
0.176 & 0 \\
0.176 & 0 \\
0.354 & 0.707 \\
-0.707 & 0 \\
0.707 & 0 \\
0 & 0 \\
0.707 & 0 \\
-0.707 & 0 \\
0 & 0
\end{bmatrix}
\begin{bmatrix} \lambda_1 \\ \lambda_2 \end{bmatrix}
\geq
\begin{bmatrix}
0.5 \\ -0.5 \\ -1.5 \\ 0.125 \\ 0.25 \\ 2.5 \\ 0.125 \\ 0.25 \\ -0.125 \\ -2.5 \\ -0.25 \\ -0.5 \\ 1.5 \\ -0.25 \\ -5.5 \\ -6.0 \\ -5.5 \\ -4.5 \\ -4.0 \\ -4.5
\end{bmatrix}.
$$

Figure 3 shows all these constraints plotted in the $\lambda_1$-$\lambda_2$ plane. The shaded area is the constraint polygon within which we are free to choose a particular value of $\lambda$.

## OPTIMAL SELECTION OF INTERNAL GRASP FORCE

An optimal selection of $\lambda$ is one for which we are furthest from violating any one of the constraints shown in figure 3. The distance of some point $\lambda_0$ from the plane formed by the $i$th constraint of equation 11 is given by

$$d_i = (\mathbf{AN})_i \lambda_0 - (\mathbf{P} - \mathbf{AC}_p)_i, \qquad (12)$$

where $(\mathbf{AN})_i$ is the $i$th row of the product $\mathbf{AN}$ and $(\mathbf{P} - \mathbf{AC}_p)_i$ is the $i$th element of $(\mathbf{P} - \mathbf{AC}_p)$. $d_i$ will be positive when $\lambda_0$ is on the permissible side of the constraint. The optimal choice of $\lambda$, $\lambda^*$, will yield the maximum value for the minimum $d_i$.

Examining the case where $\lambda$ is a scalar makes it clear how to pose this problem as a standard linear optimization problem. In figure 4a there are three points, $\lambda_1$, $\lambda_2$, and $\lambda_3$, which define bounds on $\lambda$. $\lambda$ must lie to the right of $\lambda_1$ and $\lambda_2$ and to the left of $\lambda_3$. The three lines $l_1$, $l_2$, and $l_3$ are plots of the distances

*Kerr and Roth*

Fig. 3. Constraint polygon
for example 1.



Fig. 4. Constraints on a
scalar $\lambda$.

(a)

(b)

of $\lambda$ from each of these three points. $\lambda^*$ is the desired
optimal point where the distance to the closest con-
straint point is a maximum. Figure 4b describes the
same constraints as a linear programming problem
formulated in the variables $\lambda$ and $d$ where we wish to
maximize the value of $d$ in the presence of the con-
straints $l_1$, $l_2$, and $l_3$. The variable $d$ takes on the value
$d_i$ for points that lie on $l_i$.

A general procedure for reformulating the problem
is to change equation 11 to the set of inequalities

$$d \leqslant (\mathbf{AN})_i \lambda - (\mathbf{P} - \mathbf{AC}_p)_i, \tag{13}$$

where $d$ is treated as just another variable like the
elements of $\lambda$. We wish to maximize the value of $d$
over all possible values of $d$ and $\lambda$.

These inequalities are written in more conventional
form if we create a vector $\lambda_d$ which is the vector $\lambda$
augmented with the distance variable, $d$. Equation 13
then becomes

$$[(\mathbf{AN})_i | -1] \lambda_d \geqslant (\mathbf{P} - \mathbf{AC}_p)_i,$$
$$i = 1, 2, \ldots, n_{\text{constraint}}. \tag{14}$$

The function we wish to maximize, $F(\lambda_d)$, is simply

$$F(\lambda_d) = d. \tag{15}$$

Equations 14 and 15 form a linear programming
problem in its standard form, which is readily solved
by the Simplex method.

Once a value of $\lambda$ is selected, the value of $\mathbf{C}_h$ is de-
termined from equation 4.

## 2. Manipulating Objects within the Hand

If the fingers of a hand have a sufficient number of
joints, it is possible to manipulate grasped objects rela-
tive to the palm of the hand. At the contact between
the fingertip and the object, the fingertip exerts some
type of constraint on the object. Motion of the fingers
will thus result in motion of the object. The problem
discussed in this section is that of determining the
motion of each finger joint required to achieve a de-
sired motion of the object.

The relative motion between a fingertip and the
object will be determined by the type of constraint

**8**

*Fig. 5. A finger constrained to roll on an object.*

present at the contact. If this constraint is assumed to be *point contact with friction*,[2] the problem of determining the finger motions given an object motion is relatively straightforward. Each finger can be treated as a separate manipulator which must follow the object through its motion. The motion of the contact point on each fingertip is identical to the motion of the corresponding contact point on the object. If the inverse kinematic solution for each finger is known, the required finger-joint motions are easily calculated.

In general, however, motion of the object will cause the contact point to move relative to the object's surface and relative to the fingertip's surface through some combination of rolling and sliding. Here, we will consider only the case of pure rolling between the object and the fingertip.

When the object surface and the fingertip surface roll on each other, the point of contact moves across both surfaces. The paths of the contact point across each surface will be determined by the geometry of each surface, by the motion of the object, and by the kinematics of the finger. Additionally, rolling contact represents a nonholonomic constraint between the two bodies; that is, the equations relating the motion of the object to the motion of a fingertip are expressed in terms of the velocities of the two bodies rather than in terms of the positions of the bodies (Bottema and Roth 1979).

With all these factors considered, the finger-joint angles are related to the object's position by a set of nonlinear, time-varying differential equations. Since, in general, such equations have no closed-form solution, we formulate the problem as a set of first-order differential equations suitable for numerical integration.

In order to induce a prescribed motion of the object, each fingertip must follow the object, remaining in contact, independent of the other fingers. It is therefore sufficient to examine the motion of a single finger (of sufficient generality) while it is constrained by the motion of the object. Because rolling contact allows three degrees of freedom between two bodies, a finger will require a minimum of three joints in order to
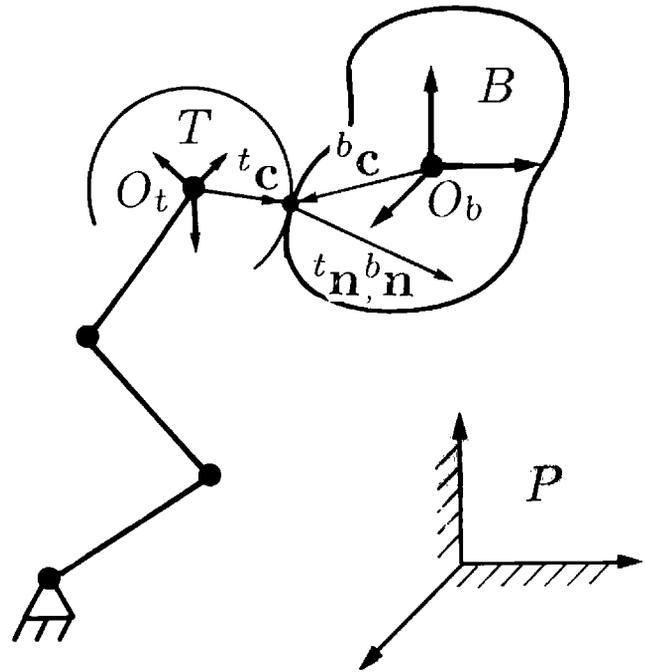
permit general motion of the body. We will consider the minimum case of fingers with three joints.

Figure 5 shows a finger in contact with an object. The motion of the object is described by the motion of point $O_b$ of frame $B$ embedded in the object and the angular velocity of $B$ with respect to the palm frame, $P$.

The rolling constraint is most easily expressed as a relationship between the velocity of point $O_b$, the angular velocity of $B$, $\omega_b$, and the finger-joint velocities, $\dot{\theta}_1$, $\dot{\theta}_2$, and $\dot{\theta}_3$. To derive this relationship, it is helpful to introduce a coordinate frame embedded in the fingertip, $T$, a vector describing the contact point with respect to $T$, $^T c$, a vector describing the contact point with respect to $B$, $^B c$, and vectors describing the common surface normal with respect to these frames, $^T n$ and $^B n$. The fingertip surface is parametrized by the variables $\alpha$ and $\beta$. Therefore, $^T n$ and $^T c$ can be described as functions of $\alpha$ and $\beta$. Similarly, the object's surface is parametrized by the variables $\eta$ and $\xi$.

In figure 5, the velocity of the contact point, $v_c$, written in terms of fingertip velocity, is

$$v_c = \dot{O}_t + \omega_t \times (T_r\, ^T c), \qquad (16)$$

---

2. Point contact with friction, for our purposes, is equivalent to replacing the contact between the two bodies with a spherical joint. The center of the spherical joint is at the point of contact.

where $\dot{\mathbf{O}}_t$ is the velocity of the origin of $T$, $\omega_t$ is the angular velocity of $T$ with respect to the palm, and $\mathbf{T}_r$ is a rotation matrix defining the orientation of $T$ with respect to $P$. This can be reformulated by first switching the order of the cross-product and then changing the cross-product to a matrix multiply using the matrix $(\mathbf{T}_r\,^T\mathbf{c})^{\otimes}$.[3]

$$\mathbf{v}_c = \dot{\mathbf{O}}_t - (\mathbf{T}_r\,^T\mathbf{c})^{\otimes}\omega_t. \tag{17}$$

$\dot{\mathbf{O}}_t$ and $\omega_t$ are found in terms of the vector of joint velocities, $\dot{\theta}$, using the Jacobian matrix for the finger, $\mathbf{J}$. The Jacobian matrix can be broken up into two parts, $\mathbf{J}_p$ and $\mathbf{J}_o$, such that

$$\dot{\mathbf{O}}_t = \mathbf{J}_p\dot{\theta} \tag{18}$$

and

$$\omega_t = \mathbf{J}_o\dot{\theta}. \tag{19}$$

Thus, finally, $\mathbf{v}_c$ can be expressed as

$$\mathbf{v}_c = [\mathbf{J}_p - (\mathbf{T}_r\,^T\mathbf{c})^{\otimes}\mathbf{J}_o]\dot{\theta} \tag{20}$$

We next describe $\mathbf{v}_c$ as a function of the velocity of the object. In a form similar to equation 17; this is

$$\mathbf{v}_c = \dot{\mathbf{O}}b - (\mathbf{B}_r\,^T\mathbf{c})^{\otimes}\omega_b, \tag{21}$$

where $\mathbf{B}_r$ is a rotation matrix describing the orientation of $B$ with respect to $P$. Equations 20 and 21 can now be combined as

$$[\mathbf{J}_p - (\mathbf{T}_r\,^T\mathbf{c})^{\otimes}\mathbf{J}_o]\dot{\theta} = \dot{\mathbf{O}}_b - (\mathbf{B}_r\,^B\mathbf{c})^{\otimes}\omega_b. \tag{22}$$

Aside from $^B\mathbf{c}$ and $^T\mathbf{c}$, the left-hand side of equation 22 is only a function of $\theta$ and $\dot{\theta}$, and the right-hand side is only a function of the position and velocity of the object.

---

3. We use the symbol $\otimes$ to indicate that the $3 \times 1$ vector $\mathbf{n}$ preceding this symbol is replaced by the $3 \times 3$ antisymmetric matrix

$$\begin{bmatrix} 0 & -n_3 & n_2 \\ n_3 & 0 & -n_1 \\ -n_2 & n_1 & 0 \end{bmatrix}.$$

The vectors $^T\mathbf{c}$ and $^B\mathbf{c}$ are functions of the surface variables $\alpha$, $\beta$, $\eta$, and $\xi$. These variables are solved for by introducing two additional properties of the contact: The contact point on the fingertip, $^T\mathbf{c}(\alpha,\beta)$, must always coincide with the contact point on the object, $^B\mathbf{c}(\eta,\xi)$, and the outward-pointing surface normal on the fingertip at the point of contact, $^T\mathbf{n}(\alpha,\beta)$, must always point in the same direction as the inward-pointing surface normal of the object, $^B\mathbf{n}(\eta,\xi)$. The first condition is written as

$$\mathbf{O}_t + \mathbf{T}_r\,^T\mathbf{c} = \mathbf{O}_b + \mathbf{B}_r\,^B\mathbf{c} \tag{23}$$

and the second as

$$\mathbf{T}_r\,^T\mathbf{n} = \mathbf{B}_r\,^B\mathbf{n}. \tag{24}$$

Rather than use equations 23 and 24 to directly eliminate the surface parameters $\alpha$, $\beta$, $\eta$, and $\xi$, we use differential forms of these equations to relate $\dot{\alpha}$, $\dot{\beta}$, $\dot{\eta}$, and $\dot{\xi}$ to the finger-joint velocities and the object's velocity. These differential relationships can be combined with equation 22 to form a complete set of differential equations which explicitly include these surface variables.

Differentiating equation 23 gives

$$\begin{aligned} \dot{\mathbf{O}}_t + \omega_t \times \mathbf{T}_r\,^T\mathbf{c} + \mathbf{T}_r\,^T\dot{\mathbf{c}} = \dot{\mathbf{O}}_b \\ + \omega_b \times \mathbf{B}_r\,^B\mathbf{c} + \mathbf{B}_r\,^B\dot{\mathbf{c}}. \end{aligned} \tag{25}$$

If equations 16 and 21 are substituted, this becomes

$$\mathbf{T}_r\,^T\dot{\mathbf{c}} = \mathbf{B}_r\,^B\dot{\mathbf{c}}. \tag{26}$$

This can be reformulated as

$$\mathbf{T}_r\mathbf{J}_{T_c}\begin{bmatrix}\dot{\alpha} \\ \dot{\beta}\end{bmatrix} = \mathbf{B}_r\mathbf{J}_{B_c}\begin{bmatrix}\dot{\eta} \\ \dot{\xi}\end{bmatrix}, \tag{27}$$

where $\mathbf{J}_{T_c}$ and $\mathbf{J}_{B_c}$ are the $3 \times 2$ Jacobian matrices of partial derivatives for the functions $^T\mathbf{c}(\alpha,\beta)$ and $^B\mathbf{c}(\eta,\xi)$. Although equation 27 forms three scalar equations in four unknowns, there are actually only two independent equations introduced. The redundant information is that equation 27 implies that the velocity of the contact point with respect to the object is equal to

zero in the direction of the surface normal. This is already implied by equation 22.

Differentiating equation 24 gives

$$\omega_t \times \mathbf{T_r}\,^T\mathbf{n} + \mathbf{T_r}\,^T\dot{\mathbf{n}} = \omega_b \times \mathbf{B_r}\,^B\mathbf{n} + \mathbf{B_r}\,^B\dot{\mathbf{n}}. \quad (28)$$

This can be rearranged to give

$$
\begin{aligned}
-(\mathbf{T_r}\,^T\mathbf{n})^{\otimes}\mathbf{J}_o\dot{\theta} + \mathbf{T_r}\mathbf{J}_{T_n}\begin{bmatrix}\dot{\alpha}\\\dot{\beta}\end{bmatrix} =\\
-(\mathbf{B_r}\,^B\mathbf{n})^{\otimes}\omega_b + \mathbf{B_r}\mathbf{J}_{B_n}\begin{bmatrix}\dot{\eta}\\\dot{\xi}\end{bmatrix},
\end{aligned}
\quad (29)
$$

where $\mathbf{J}_{T_n}$ and $\mathbf{J}_{B_n}$ are the Jacobian matrices for the vector functions $^T\mathbf{n}(\alpha,\beta)$ and $^B\mathbf{n}(\eta,\xi)$. This forms another set of three equations in four variables, but again one is redundant because only two equations are required to specify the direction of a normal vector; the redundancy comes from assuming that the magnitude of the normal vectors is 1.

Together, equations 27 and 29 form four independent equations in the four variables $\alpha$, $\beta$, $\eta$, and $\xi$. These four, along with equation 22, form a complete set of first-order differential equations in seven variables. All these equations can be combined in the single vector differential equation

numerically integrate equation 30 is with a forward differencing method, where both sides of the equation are multiplied by the inverse of $\mathbf{M}$ at each step of the integration. Because $\mathbf{M}$ is of dimensions $9 \times 7$, the right generalized inverse[4] of $\mathbf{M}$ must be used.

## 3. Hand Workspaces

The final topic of this paper deals with determining the range of possible manipulations with a given hand. This range, which generally is a six-dimensional quantity, defines the *workspace* of the hand. The workspace will be a function of the rolling or sliding that occurs at the contacts, the configuration of the contact points on the object and on the fingertips, the shape of the object and of the finger links, and the kinematic structure of each of the fingers.

To simplify this problem, we will work under the following assumptions:

The type of contact present between the fingertips and the object is considered to be point contact with friction, and the contact points do not change during the motion.

$$
\begin{bmatrix}
\mathbf{J}_p - (\mathbf{T_r}\,^T\mathbf{c})^{\otimes}\mathbf{J}_o & 0 & 0\\
0 & \mathbf{T_r}\mathbf{J}_{T_c} & -\mathbf{B_r}\mathbf{J}_{B_c}\\
-(\mathbf{T_r}\,^T\mathbf{n})^{\otimes}\mathbf{J}_o & \mathbf{T_r}\mathbf{J}_{T_n} & -\mathbf{B_r}\mathbf{J}_{B_n}
\end{bmatrix}
\begin{bmatrix}\dot{\theta}\\\dot{\alpha}\\\dot{\beta}\\\dot{\eta}\\\dot{\xi}\end{bmatrix}
=
\begin{bmatrix}
\mathbf{I} & -(\mathbf{B_r}\,^B\mathbf{c})^{\otimes}\\
0 & 0\\
0 & -(\mathbf{B_r}\,^B\mathbf{n})^{\otimes}
\end{bmatrix}
\begin{bmatrix}\dot{\mathbf{O}}_b\\\omega_b\end{bmatrix},
\quad (30)
$$

or as

$$\mathbf{M}\dot{\theta}' = \mathbf{R}\mathcal{V}_b.$$

The vector $\dot{\theta}'$ is equal to $\dot{\theta}$ augmented with the derivative of each of the surface parameters, and $\mathcal{V}_b$ is known as the generalized velocity of the object. $\mathbf{M}$ is a $9 \times 7$ matrix and $\mathbf{R}$ is a $9 \times 6$ matrix. $\mathbf{M}$ and $\mathbf{R}$ are functions of the configuration of the finger, the orientation of the object, and the location of the contact point on the finger and object surfaces.

Equation 30 is a nonlinear, time-varying ordinary differential equation which, in general, will not have a closed-form solution. The most straightforward way to

The hand workspace will be defined for a particular configuration of contact points on the object and for particular locations of the contact points on the fingertips.

The workspace for each fingertip[5] is known and is considered fixed relative to the palm of the hand.

---

4. The right generalized inverse of $\mathbf{M}$ is defined as $\mathbf{M}^T\mathbf{M})^{-1}\mathbf{M}^T$. If the nine scalar equations of eq. 30 are not conflicting, this generalized inverse will give the correct solution for $\dot{\theta}'$.

5. The workspace for a fingertip is defined as the volume of points reachable by the contact point on the fingertip, given the kinematic constraints on the motion of the fingertip relative to the finger base.

Fig. 6. An object located
with respect to three fingertip
workspaces.

*Fig. 7. An object at several
points in the workspace.*
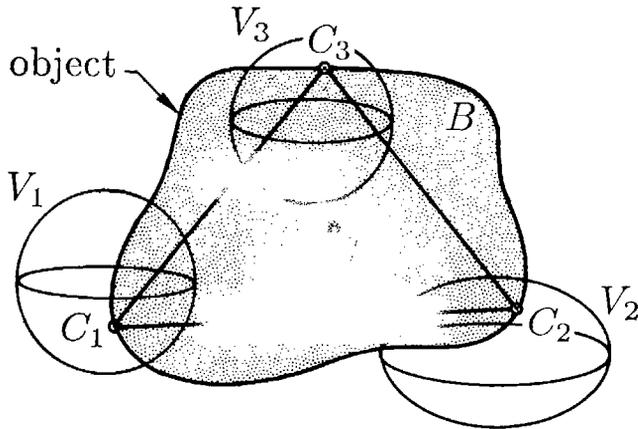
Collisions or intersections between the object and
the finger links or between the finger links them-
selves will be ignored.

With these four assumptions, determining the work-
space for a hand can be reduced to the problem illus-
trated in figure 6 for a three-fingered hand. The work-
space is defined by all possible configurations of the
object relative to the palm such that each of the con-
tact points on the object, $c_i$, lies within its respective
finger workspace $V_i$.

Rather than deal with the complete six-dimensional
configuration space of the object, we will define the
*total workspace* of the hand as the volume swept out
by one particular point $q$ fixed in the object as the
object is moved through all possible configurations.
For our purposes, we will choose $q$ to be the spatial
center of the contact points on the object.

In this section we will determine constructions for
the boundary of the total workspace for two-fingered
planar hands with circular fingertip workspace bound-
aries, and for spatial, three-fingered hands with spheri-
cal fingertip workspace boundaries.

## PLANAR-HAND WORKSPACES

Figure 7 shows a two-fingered hand grasping an object
at several points in the workspace. The finger work-
spaces, $V_1$ and $V_2$, are bounded by the curves $\mathcal{U}_1$ and
$\mathcal{U}_2$, respectively. In figure 7a, neither finger is at the
boundary of its own workspace. In 7b, one finger is at

**12**

its boundary, but point $q$ is not at the hand-workspace boundary, $\mathcal{W}$. In 7c, again only one finger is at its boundary, but here $q$ *is* at the workspace boundary. In 7d, both fingers are at their boundaries and $q$ is at the workspace boundary. This series of figures illustrates how the boundary of the workspace for a two-fingered, planar hand is developed.

In general, the bounding curve of the total hand workspace, $\mathcal{W}$, will be made up of three different sections. The first section, $\mathcal{S}_1$, is formed when the contact point $C_1$ lies on the boundary $\mathcal{U}_1$. $\mathcal{S}_1$ will be formed by the locus of $q$ when the points $q$, $C_1$ and the center of $\mathcal{U}_1$, $O_1$, are collinear. Figure 8 shows that $\mathcal{S}_1$ is made up of two circles concentric with $\mathcal{U}_1$. One circle will be of radius $d + r_1$, and the other of radius $d - r_1$. If $d - r_1 < 0$, the inner circle will not actually form a part of the workspace boundary, because points inside it are accessible when $C_1$ lies *within* $\mathcal{U}_1$.

The second section of $\mathcal{W}$, $\mathcal{S}_2$, will be formed in a manner similar to $\mathcal{S}_1$ when $C_2$ lies on the boundary $\mathcal{U}_2$. $\mathcal{S}_1$ and $\mathcal{S}_2$ correspond to one of the contacts lying at its boundary, without concern for the other finger's limitations. The total workspace of the hand will be a subset of the intersection of the areas bounded by $\mathcal{S}_1$ and $\mathcal{S}_2$.

The third section of $\mathcal{W}$, $\mathcal{S}_3$, is generated when both contact points lie on their respective boundaries, $\mathcal{U}_1$ and $\mathcal{U}_2$, as in figure 9. In general, this curve may not bound the workspace, but in some cases $\mathcal{S}_3$ will be

tangent to $\mathcal{S}_1$ and $\mathcal{S}_2$ at various points. These points will break $\mathcal{S}_3$ into several segments. The boundary for the total workspace is then formed by piecing together the appropriate segments of $\mathcal{S}_1$, $\mathcal{S}_2$, and $\mathcal{S}_3$.

If $\mathcal{U}_1$ and $\mathcal{U}_2$ are circles, the section $\mathcal{S}_3$ is formed by the coupler curve of the four-bar mechanism $O_1 C_1 C_2 O_2$, where the link $C_1 C_2$ forms the coupler and the link $O_1 O_2$ is stationary. Point $q$ on the coupler traces out the appropriate coupler curve.

Figure 10 shows the possible types of four-bar linkages for generating topologically different workspaces for two-fingered hands with circular finger workspaces. The workspaces are classified according to whether the four-bar mechanism $O_1 C_1 C_2 O_2$ meets the Grashof criteria,[6] according to which link of the mechanism is shortest for Grashof-type linkages, and according to whether the sections $\mathcal{S}_1$ and $\mathcal{S}_2$ have an inner circle forming part of the boundary. The appropriate segments of $\mathcal{S}_1$, $\mathcal{S}_2$, and $\mathcal{S}_3$ which form $\mathcal{W}$ were chosen by examining each segment of each curve to verify that it is actually a segment defining the boundary of the total workspace.

## SPATIAL-HAND WORKSPACES

The workspace for a three-fingered, spatial hand can be developed in a manner similar to that for the two-

---

6. The Grashof criteria states that if the sum of the lengths of the shortest and longest links of a planar four-bar mechanism is less than or equal to the sum of the lengths of the two other links, then the shortest link will be able to rotate 360° with respect to the other links.

Non-Grashof linkage
$|C_1 q| > |O_1 C_1|, |C_2 q| > |O_2 C_2|$

Non-Grashof linkage
$|C_1 q| > |O_1 C_1|, |C_2 q| < |O_2 C_2|$

Non-Grashof linkage
$|C_1 q| < |O_1 C_1|, |C_2 q| < |O_2 C_2|$

Grashof linkage
Shortest link: $O_2 C_2$
$|C_1 q| < |O_1 C_1|, |C_2 q| > |O_2 C_2|$

Grashof linkage
Shortest link: $C_1 C_2$
$|C_1 q| < |O_1 C_1|, |C_2 q| < |O_2 C_2|$

Grashof linkage
Shortest link: $O_1 O_2$
$|C_1 q| < |O_1 C_1|, |C_2 q| < |O_2 C_2|$

Grashof linkage
Shortest link: $O_2 C_2$
$|C_1 q| < |O_1 C_1|, |C_2 q| < |O_2 C_2|$

Grashof linkage
Shortest link: $O_1 O_2$
$|C_1 q| > |O_1 C_1|, |C_2 q| < |O_2 C_2|$



fingered, planar case. For a hand with three fingers, $\mathcal{W}$ is made up of seven different sections. The first three sections, $\mathscr{S}_1$, $\mathscr{S}_2$, and $\mathscr{S}_3$, are formed when only one of the contacts, $C_1$, $C_2$, or $C_3$, lies at its finger-workspace boundary. For instance, $\mathscr{S}_1$ is the surface formed when $C_1$ lies on the boundary $\mathcal{U}_1$ and the boundaries $\mathcal{U}_2$ and $\mathcal{U}_3$ are ignored.

For fingers with spherical workspace boundaries, each of these first three sections will consist of an outer sphere of radius $d_i + r_i$ and possibly an inner sphere of radius $d_i - r_i$. The inner sphere will be part of $\mathscr{S}_i$ if $d_i - r_i > 0$, as shown in figure 11. The total workspace of the hand will be a subset of the intersection of the volumes bounded by $\mathscr{S}_1$, $\mathscr{S}_2$, and $\mathscr{S}_3$.

The next three sections of $\mathcal{W}$, $\mathscr{S}_4$, $\mathscr{S}_5$, and $\mathscr{S}_6$, are formed when two of the contacts lie on their respective boundaries and the third boundary is ignored. For example, $\mathscr{S}_4$ is the surface formed when $C_2$ lies on $\mathcal{U}_2$, $C_3$ lies on $\mathcal{U}_3$, and $\mathcal{U}_1$ is ignored. The surfaces of this second set are more difficult to visualize. If two of the contact points, $C_i$ and $C_j$, are confined to the surfaces $\mathcal{U}_i$ and $\mathcal{U}_j$, the object is still free to move with four degrees of freedom, and $q$ will sweep out a volume. $\mathscr{S}_k$ is the surface bounding this volume. The boundary can be determined by noting that when $q$ lies at the bounding surface it can move with only two degrees of freedom locally.

*Fig. 12. Surface $\mathcal{S}_k$ of a
spatial workspace. The
cross-section shown forms
two coupler curves. The
circles indicate that the $\mathcal{S}_k$ is
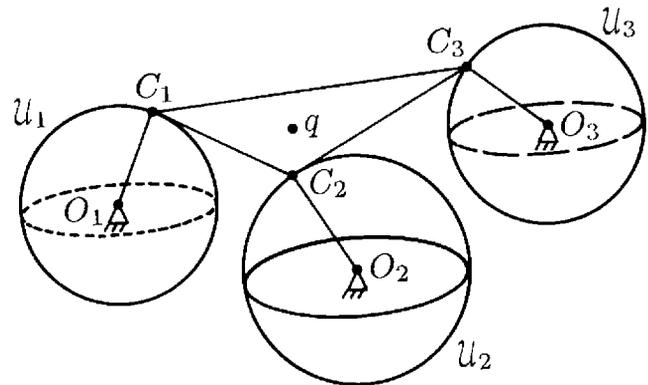the surface of revolution
formed by these curves.*

*Fig. 13. A mechanism for
forming $\mathcal{S}_7$.*
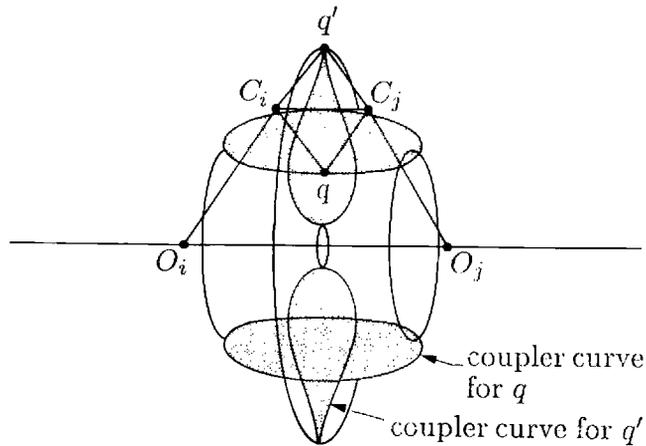




In the case where $\mathcal{U}_i$ and $\mathcal{U}_j$ are spheres, $\mathcal{S}_k$ is formed by the locus of points $q$ when the points $O_i$, $O_j$, $C_i$, $C_j$, and $q$ are all coplanar. This condition will define the surface $\mathcal{S}_k$ for $k = 1,2,3$; $i \neq j \neq k$. When all these points are coplanar, as shown in figure 12, we get $q$ tracing out the coupler curve for a four-bar linkage in the plane formed by the four points. The surface $\mathcal{S}_k$ is then formed by rotating the coupler curve about the line $O_iO_j$. Because point contact with friction will allow the object to rotate about the line $C_iC_j$, $\mathcal{S}_k$ will be formed by the revolution of two distinct coupler curves: one where $q$ is on the far side of the line $C_iC_j$ from the points $O_i$ and $O_j$, and one where $q$ lies on the near side.

The last section of $\mathcal{W}$, $\mathcal{S}_7$, is formed when all three of the fingertips move on their respective workspace boundaries. In this situation, the object will still be able to move with three degrees of freedom, and, in general, point $q$ will sweep out a volume. The desired surface, $\mathcal{S}_7$, is the surface bounding this volume. $\mathcal{S}_7$ can be formed by the equivalent mechanism shown in figure 13, where each joint is a spherical joint. When $q$ lies on $\mathcal{S}_7$, it will only be able to move locally with two degrees of freedom. This defines a singular condition for the mechanism from which $\mathcal{S}_7$ can be determined.

The total hand-workspace boundary will be made up of pieces of all seven surfaces, $\mathcal{S}_1$ through $\mathcal{S}_7$. These surfaces will intersect along curves which break each surface up into patches. $\mathcal{W}$ is formed by examining each patch and piecing together only those patches that form the actual workspace boundary.

## 4. Discussion

### INTERNAL GRASP FORCES

The method presented here is a systematic way of determining a set of internal grasp forces that will yield a stable grasp. The constraint polygon characterizes the properties of the grasp. If it is large, there will be a wide range of possible internal grasp forces and the grasp will be relatively easy to achieve. If the constraints overlap such that no proper polygon is formed at all, it will be impossible to grasp the object in the given configuration. In general, the optimal value of $d$ from equation 15 will be inversely proportional to the grasp difficulty; negative values of $d$ correspond to impossible grasp configurations.

In addition to the friction and joint-torque limit constraints, other types of constraints can be handled with this procedure. For example, it may be desirable to limit the magnitude of the contact forces to fall within the range of tactile or force sensors. It may also be necessary to limit the contact normal forces to prevent crushing the object. These types of constraints can also be formulated as inequalities bounding the value of $C$ and can thus be included in the matrix inequality of equation 10.

Types of contact constraints other than the one explicitly dealt with here may also be considered. For example, if the friction properties at the contact are not uniform in the tangential directions, as in the case of contact with the edge of an object, the friction constraints of equations 7 and 8 can be modified to reflect such conditions.

*Kerr and Roth*      **15**

## Manipulating Objects

For fingertip surfaces and object surfaces of typical complexity, it will be necessary to numerically integrate equation 30 to find the finger-joint motions as a function of the object motion. It is possible to contrive cases where the fingertip has a fixed orientation and where the surfaces are extremely simple; for these examples, a closed-form solution is possible. These situations, however, are unlikely to arise in practice.

When the object surface and the fingertip surfaces are geometrically simple, such as planes, spheres, or cylinders, it is possible to eliminate the surface variables $\alpha$, $\beta$, $\eta$, and $\xi$ directly (Kerr 1984). This elimination will allow the simpler set of three equations, 22, to be used instead of equation 30.

This problem can also be simplified if tactile sensors can be used to measure the location of the contact points on the fingertips directly. If such a measurement is available, again the simpler set of equations, 22, can be used (Kerr 1984).

## Hand Workspaces

We have shown, for a restricted set of hands, how to generate the boundary for the total hand workspace. Unfortunately, even for this highly simplified problem, the solution has proved rather complex. For actual hands with irregularly shaped workspaces, it is likely that numerical methods will be the best way to determine the total workspace.

The treatment of this problem here has not addressed many of the important issues relating to the workspace. The first of these is the range of orientations possible at each point in the total workspace. One possible way to deal with the orientations is to determine the minimum range of orientations possible about any axis for each point in the total workspace. Other workspaces which are subsets of the total workspace could be formed for which a minimum range of orientations is possible at all points in the workspace. These additional workspace descriptions would be useful in planning tasks where the orientation of the object relative to the palm is specified.

The analysis here assumes that the contact points are fixed on both the fingertips and the object. If the contact points are allowed to move across the surfaces through rolling or sliding, it is possible to increase the size of the workspace greatly. This is particularly noticeable when rolling small objects between the fingertips — very large changes of orientation are possible. Unfortunately, with rolling or sliding considered, the extent of the workspace will be a function of the initial configuration of the object in the hand and of the path it moves along.

The last important point not addressed above is that of intersection between the object and the fingers and between the fingers themselves. In most instances, collisions within the hand will be the actual limiting factor on the extent of the workspace. Characterizing the workspace with this consideration is very difficult.

We have addressed three of the fundamental problems encountered when manipulating objects within a multifingered, articulated hand. Although some of the analysis has been limited to the specific kinds of hands considered, the methods are useful for approaching more general situations.

## Acknowledgments

### References

Bottema, O., and B. Roth. 1979. *Theoretical Kinematics*. Amsterdam: North-Holland.

Hanafusa, H., and H. Asada. 1977. Stable prehension by a robot hand with elastic fingers. *Proc. 7th ISIR,* Tokyo, pp. 361–368.

Hollerbach, J. 1982. Workshop on the design and control of dexterous hands. MIT AI memo 661.

Kerr, J. R. 1984. An analysis of multi-fingered hands. Ph.D. thesis, Stanford University Dept. of Mechanical Engineering.

Holzmann, W., and J. M. McCarthy. 1985. Computing frictional forces associated with a three-fingered grasp. *Proc. of the 1985 IEEE Conference on Robotics and Automation,* St. Louis, pp. 594–600.

Ohwovoriole, M. S. 1980. An extension of screw theory and its application to the automation of industrial assemblies.

Ph.D. thesis, Stanford University Dept. of Mechanical Engineering.

Roth, B. 1975. Performance evaluation of manipulators from a kinematic viewpoint. In *Performance Evaluation of Programmable Robots and Manipulators.* Washington, D.C.:NBS.

Salisbury, J. K., and J. J. Craig. 1981. Articulated hands: Force control and kinematic issues. *Int. J. Robotics Res.* 1(1):4–17.

Salisbury, J. K. 1982. Kinematic and force analysis of articulated hands. Ph.D. thesis, Stanford University Dept. of Mechanical Engineering.

Strang, G. 1976. *Linear algebra and its applications.* New York: Academic.